

An optical study of the GRB 970111 field beginning 19 hours after the Gamma-Ray Burst ^{*,**,***}

J. Gorosabel¹, A. J. Castro-Tirado^{1,2}, C. Wolf³, J. Heidt⁴, T. Seitz^{4,5}, E. Thommes⁶, C. Bartolini⁷, A. Guarnieri⁷, N. Masetti^{7,8}, A. Piccioni⁷, S. Larsen⁹, E. Costa¹⁰, M. Feroci¹⁰, F. Frontera¹¹, E. Palazzi⁸, and N. Lund¹²

¹ Laboratorio de Astrofísica Espacial y Física Fundamental (LAEFF-INTA), P.O. Box 50727, E-28080 Madrid, Spain.

² Instituto de Astrofísica de Andalucía (IAA-CSIC), P.O. Box 03004, E-18080 Granada, Spain.

³ Max-Planck-Institut für Astronomie, Heidelberg, Germany.

⁴ Landessternwarte Heidelberg, Königstuhl, 69117 Heidelberg, Germany.

⁵ Lehrstuhl für Ergonomie, Technische Universität München, Boltzmannstr. 15, 85747 Garching, Germany.

⁶ Royal Observatory, Blackford Hill, Edinburgh Hill, Edinburgh EH9 3HJ, United Kingdom.

⁷ Dipartimento di Astronomia, Università di Bologna, Via Zamboni 33, I-40126 Bologna, Italy.

⁸ Istituto Tecnologie e Studio Radiazioni Extraterrestri, CNR, Bologna, Italy.

⁹ Niels Bohr Institute for Astronomy, Physics and Geophysics, Copenhagen University Astronomical Observatory, Julian Maries Vej 30, 2100 Copenhagen, Denmark.

¹⁰ Istituto di Astrofisica Spaziale, CNR, Roma, Italy.

¹¹ Dipartimento di Fisica, Università di Ferrara, Ferrara, Italy.

¹² Danish Space Research Institute, Copenhagen, Denmark.

Received date; accepted date

Abstract. We present the results of the monitoring of the GRB 970111 field that started 19 hours after the event. This observation represents the fastest ground-based follow-up performed for GRB 970111 in all wavelengths. As soon as the detection of the possible GRB 970111 X-ray afterglow was reported by Feroci et al. (1998) we reanalyzed the optical data collected for the GRB 970111 field. Although we detect small magnitude variability in some objects, no convincing optical counterpart is found inside the WFC error box. Any change in brightness 19 hours after the GRB is less than 0.2 mag for objects with B < 21 and R < 20.8.

The bluest object found in the field is coincident with 1SAX J1528.8+1937. Spectroscopic observations revealed that this object is a Seyfert-1 galaxy with redshift $z = 0.657$, which we propose as the optical counterpart of the X-ray source.

Further observations allowed to perform multicolour photometry for objects in the GRB 970111 error box. The colour-colour diagrams do not show any object with unusual colours. We applied a photometric classification method to the objects inside the GRB error box, that can distinguish stars from galaxies and estimate redshifts. We were able to estimate photomet-

ric redshifts in the range $0.2 < z < 1.4$ for several galaxies in this field and we did not find any conspicuous unusual object.

We note that GRB 970111 and GRB 980329 could belong to the same class of GRBs, which may be related to nearby sources ($z \sim 1$) in which high intrinsic absorption leads to faint optical afterglows.

Key words: Gamma rays: bursts - Galaxies: Seyfert

1. INTRODUCTION

Gamma-Ray Bursts (GRBs) are powerful brief transient phenomena of high-energy radiation that appear randomly in the sky. They were first detected in 1969 by the *Vela* satellites (Klebesadel et al. 1973) and have remained for many years one of the most elusive mysteries in astrophysics.

Before the launch of the *BeppoSAX* and *RossixTE* satellites in 1996, they had not been detected in any other wavelength region, and their distance scale remained unknown. The discovery of X-ray afterglows by both satellites revolutionized the field, because they are able to provide very accurate GRB error boxes within a few hours (circular error boxes with radius up to 50''), which enables very rapid follow up observations at longer wavelengths. Eight GRBs detected by *BeppoSAX* have been detected at optical and infrared wavelengths; GRB 970228 (Guarnieri et al. 1997a, van Paradijs et al. 1997), GRB 970508 (Bond 1997, Djorgovski et al. 1997, Castro-Tirado et al. 1998a), GRB 971214 (Halpern et al. 1997, Gorosabel et al. 1998, Ramaprakash et al. 1998), GRB 980326 (Groot et al. 1998), GRB 980329 (Klose 1998, Palazzi et al. 1998a, 1998b,

Send offprint requests to: J. Gorosabel (jgu@laeff.esa.es)

* Based on observations collected at the German-Spanish Astronomical Center, Calar Alto, operated by the Max-Planck-Institut für Astronomie, Heidelberg, jointly with the Spanish National Commission for Astronomy.

** Based on observations carried out at the Danish 1.54-m Telescope on the European Southern Observatory, La Silla, Chile

*** Based on observations at the Osservatorio Astronomico di Loiano, Italy.

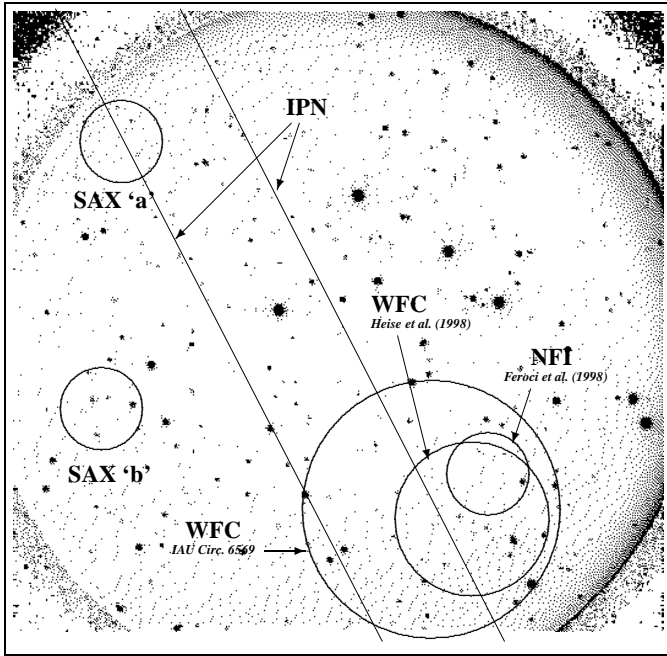


Fig. 1. The B band image of GRB 970111 taken 19 hours after the event. The circular field of view has a radius of $8'$. The largest circle (radius $3'$) represents the 3σ WFC error circle reported by in't Zand et al. (1997), later refined by Heise et al. (1998) with a radius of $1'.8$. The small circle inside the WFC error box is the $60''$ radius error box (confidence level 90%) given by the NFI for the possible X-ray afterglow of GRB 970111. The improved IPN annulus is also shown (Galama et al. 1997). The NFI error circle is only marginally consistent with the IPN annulus. On the other hand, the two 3σ X-ray error boxes sources detected by SAX, labeled SAX “a” and SAX “b” (Butler et al. 1997) are shown. North is at the top and east to the left.

Taylor et al. 1998), GRB 980519 (Jaunsen et al. 1998, Maury et al. 1998), GRB 980613 (Hjorth et al. 1998, Djorgovski et al. 1998a, 1998b), and GRB 980703 (Frail et al. 1998, Zapatero-Osorio et al. 1998).

Spectral information taken for GRB 970508 showed that the gamma event occurred at a redshift $z \geq 0.83$, therefore supporting the cosmological origin of GRBs (Metzger et al. 1997). Recently, Kulkarni et al. (1998) measured the redshift of the host-galaxy of GRB 971214 ($z=3.42$), placing it at a distance of ~ 12 billion light years (assuming the universe to be about 14 billion years old). This large distance implies an energy release at least of $\sim 3 \times 10^{53}$ erg, which can not be explained by the neutron star merger model, at least in its simplest form (Narayan et al. 1992).

GRB 970111 was the first GRB observed by *BeppoSAX* that was promptly followed up at other wavelengths. In fact, the results presented in this paper represent the fastest follow-up observation performed for GRB 970111 in all wavelengths. It was detected as a three-peak Gamma-Ray Burst on January 11, 1997 by the Wide Field Camera of the X-ray *Beppo-*

poSAX satellite (Costa et al. 1997). The burst was localized at $\alpha = 15^h 28^m 24^s$, $\delta = +19^\circ 40.0'$ (equinox 2000.0; error box radius = $10'$). Soon after that, Butler et al. (1997) reported the presence of two faint X-ray sources in the field of GRB 970111; 1SAX J1528.8+1944 and 1SAX J1528.8+1937, labeled as “a” and “b” respectively. Then, Hurley et al. (1997a) reduced the error box of GRB 970111 by means of the *Ulysses* and BATSE data, and found that only the *BeppoSAX* source “a” lied within it. Unfortunately, due to a misalignment of the Wide Field Cameras of *BeppoSAX* (in't Zand et al. 1997), the error box reported by Costa et al. (1997) had to be shifted of $\sim 4'.2$ from its previous position. The new error box provided by Hurley et al. (1997b), seven times smaller than the former, placed both X-ray sources far away ($\sim 10' - 15'$) from this new error box, thus showing both sources to be unrelated to GRB 970111. 1SAX J1528.8+1944 has been detected by ROSAT (Voges et al. 1997) and it was found to be related to the variable radio source VLA J1528.7+1945 (Frail et al. 1997). An optical spectrum revealed two objects that lied within $1''$ from VLA J1528.7+1945, showing redshifts $z \sim 0.636$ and $z \sim 0.458$, respectively (Kulkarni et al. 1997). Frontera et al. (1997) provided more precise coordinates for this X-ray source, however no object showed remarkable variations in the optical, neither in the field of GRB 970111 nor in the error boxes of the two X-ray sources (Guarnieri et al. 1997b). Radio observations at 840 MHz, 1.4 GHz and 1.5 GHz carried out between 26.4 hours and 120 days did not reveal any steady source in the intersection between the WFC $3'$ error box with a new improved IPN annulus (Galama et al. 1997a, Galama et al. 1997b). One month after the event, the error box was scanned by the BIMA array at 3.5 mm, without detecting any fading source at millimeter wavelengths (Smith et al. 1997). Very recently the WFC team improved again the error box to an irregular circle of $1'.8$ radius, still consistent with the previous one (Heise et al. 1998). Furthermore a recent reanalysis of the MECS data revealed a previously unknown X-ray source, 1SAX J1528.1+1937, which is almost entirely contained within the 3σ WFC error box (Feroci et al. 1998). However this source is only marginally consistent with the last IPN annulus reported by Galama et al. (1997b). The above mentioned new γ -ray and X-ray positions of the GRB 970111 encouraged us to reanalyze the results already presented elsewhere (Castro-Tirado et al. 1998b). Furthermore new observations were carried out, which enabled us to observe the GRB 970111 up to 6 months after the gamma-ray event. Section §2 will briefly describe the data reduction and calibration techniques, while Section §3 will present and discuss the results. Finally, Section §4 will draw the conclusions.

2. Observations

Observations were obtained with the 2.2-m telescope at the Calar Alto Spanish-German observatory (hereafter CAHA), the 1.5-m Telescope of the Bologna Astronomical Observatory and with the 1.54-m Danish Telescope at La Silla observatory. Tables 1, 2 and 3 display the observing logs for the WFC error

Table 1. Log of observations covering the WFC 970111 position.

Date of 1997	Exposure time (Ks)							Telescope
	U	B	V	R	i	z	free	
Jan. 12	-	1.5	-	0.6	-	-	-	2.2 CAHA
Jan. 17	-	2.7	-	0.9	-	-	-	1.5 Loiano
Feb. 10	-	1.5	-	0.6	-	-	-	2.2 CAHA
Feb. 11	-	-	-	0.6	-	-	-	2.2 CAHA
Mar. 5	-	-	-	1.8	-	-	-	1.5 Loiano
Mar. 10	0.6	0.6	-	0.6	0.6	0.6	-	1.54 Danish
Mar. 12	-	1.8	-	-	-	-	-	1.54 Danish
Mar. 14	-	-	-	-	-	-	7.2	1.54 Danish
Mar. 15	-	3.6	-	-	-	-	-	1.54 Danish
Jun. 26	-	-	4.8	-	-	-	-	1.54 Danish
Jun. 27	-	-	-	3.2	-	-	-	1.54 Danish
Jul. 1	-	2.7	-	-	-	-	-	1.54 Danish
Jul. 3	-	-	-	1.8	1.6	-	-	1.54 Danish
Jul. 4	-	-	-	-	2.9	-	-	1.54 Danish
$0.17^h+7.42^h+3.37^h+4.89^h+1.42^h+0.17^h+2^h$								$= 19.42^h$

Table 2. Log of observations covering the field of source 1SAX J1528.8+1944.

Date of 1997	Exposure time (Ks)							Telescope
	U	B	V	R	i	z	free	
Jan. 12	-	1.5	-	0.6	-	-	-	2.2 CAHA
Jan. 14	-	1.2	-	1.2	-	-	-	1.5 Loiano
Jan. 17	-	2.7	-	0.9	-	-	-	1.5 Loiano
Jan. 31	-	3.0	1.2	0.9	-	-	-	1.5 Loiano
Feb. 10	-	1.5	-	0.6	-	-	-	2.2 CAHA
Feb. 11	-	-	-	0.6	-	-	-	2.2 CAHA
Feb. 14	-	-	1.8	-	-	-	-	1.5 Loiano
Feb. 17	-	-	1.62	1.8	-	-	-	1.5 Loiano
Feb. 18	-	4.5	2.7	1.8	-	-	-	1.5 Loiano
Mar. 5	-	-	-	1.8	-	-	-	1.5 Loiano
Mar. 13	-	3.6	-	1.8	-	-	-	1.5 Loiano
$5.0^h+2.03^h+3.33^h$								$= 7.03^h$

Table 3. Log of observations covering the field of source 1SAX J1528.8+1937.

Date of 1997	Exposure time (Ks)							Telescope
	U	B	V	R	i	z	free	
Jan. 12	-	1.5	-	0.6	-	-	-	2.2 CAHA
Jan. 14	-	1.2	-	1.2	-	-	-	1.5 Loiano
Feb. 10	-	1.5	-	0.6	-	-	-	2.2 CAHA
Feb. 11	-	-	-	0.6	-	-	-	2.2 CAHA
$1.17^h + 0.83^h$								$= 2^h$

box (in't Zand et al. 1997), and the two SAX X-ray sources labeled "a" and "b".

Table 4. Filters used in the observations carried out at La Silla.

Filter name	ESO filter number	Central wavelength (nm)	Band-width FWHM (nm)	Maximum transmission (%)
Bessel U	632	355.60	53.37	66
Bessel B	450	443.57	102.29	67
Bessel V	451	544.80	116.31	85
Bessel R	452	648.87	164.7	85
Gunn i	425	797.79	142.88	85
Gunn z	462	903.35		

2.1. Observations at CAHA

We obtained B and R band images on January 12, starting 19 hours the gamma-ray event. The frames were obtained at the 2.2-m telescope at CAHA equipped with the Calar Alto Faint Object Spectrograph (CAFOS). The detector used is a 2048×2048 pixel CCD providing a scale of 0.53 arc sec pixel $^{-1}$. The limiting magnitudes of these images are $B \sim 23.7$, $R \sim 23.0$.

As it is shown in Fig. 1, the large field of view provided by CAFOS ($16'$ in diameter) enabled us to image all the improved positions reported in the literature (Butler et al. 1997, Hurley et al. 1997a, 1997b, Galama et al. 1997b, in't Zand et al. 1997, Feroci et al. 1998, Heise et al. 1998) as well as the X-ray sources 1SAX J1528.8+1944 and 1SAX J1528.8+1937. Additional comparison B and R frames were taken on February 10 and 11. We searched for variables objects located inside the 1SAX J1528.8+1944, 1SAX J1528.8+1937 and the GRB error box comparing the images taken in both filters on January 12 with those taken on February 10 and 11. The results are discussed in § 3.1.

2.2. Observations at Loiano

We used the 1.5-m telescope (equipped with the Bologna Faint Object Spectrograph and Camera, hereafter BFOSC) at the Bologna Astronomical Observatory, on January 14-15, 17 and 31, on February 14, 17-18 and on March 5 and 13. The detector used with BFOSC is a 2048×2048 CCD, with a scale of about 0.5 arc sec pixel $^{-1}$. B and R band filters were usually used, sometimes V band images were also taken. Frames were also obtained on February 19, but the seeing was very poor and the frames had a low S/N ratio; therefore, they were not used in this work. Long exposures times were used to reach a limiting magnitude of at least ~ 21 for each frame. B,V and R images of the PG 1047+003 sequence (Landolt 1992) were taken, in order to calibrate the field of GRB 970111.

2.3. Observations at La Silla

The observations were performed during two observing runs on the Danish 1.54-m telescope at ESO La Silla Observatory, the first one in March 1997, and the second one in June-July 1997. The Instrument used was the Danish Faint Object Spectrograph and Camera (DFOSC), providing a field of view

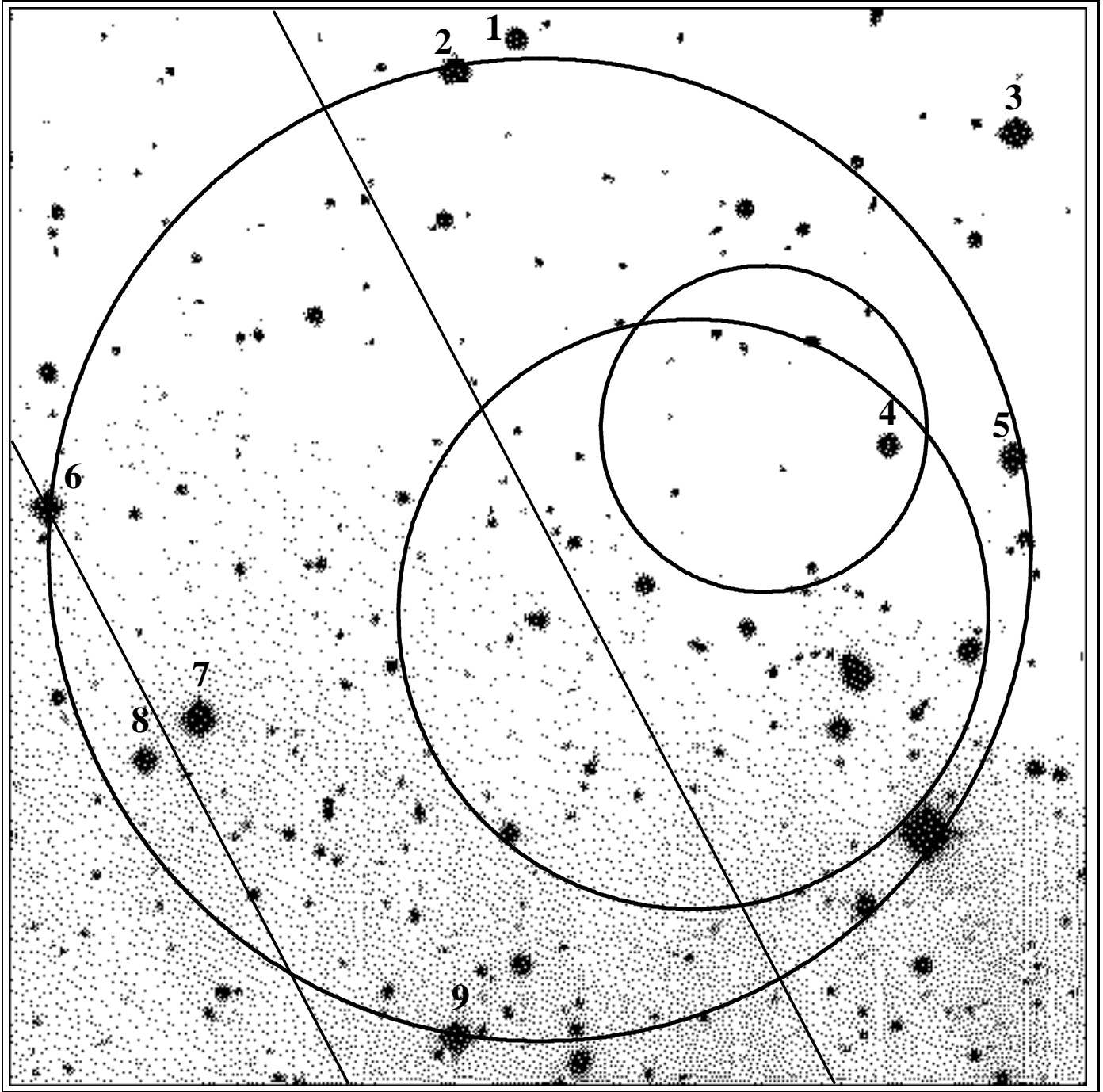


Fig. 2. Combination of BVR (Bessel) and *i* (gunn) images taken at La Silla for GRB 970111 field. The images includes the two WFC circles (in't Zand et al. 1997, Heise et al. 1998) and the NFI error box (Feroci et al. 1998). The straight lines represent the IPN annulus (Galama et al. 1997b). The total exposure time amounts to 19 hours. The field of view is $6'.6 \times 6'.6$. North is at the top and east to the left.

of $13'.6 \times 13'.6$. The CCD was a backside illuminated Loral/Lessler chip with 2052×2052 $15 \mu m$ pixels. Observations were made using U,B,V,R-Bessel and *i*,z-gunn filters (see Table 4).

Table 5 shows the magnitudes of the nine stars labeled in Fig. 2. Photometric calibrations were performed observing

the Landolt field #98 (Landolt 1992) under photometric conditions at different air masses and filters, resulting the following absorption coefficients: $K_U = 0.47$, $K_B = 0.23$, $K_V = 0.13$, $K_R = 0.09$, $K_i = 0.05$. The 1σ limiting magnitude of the co-added frames are: U=20, B=24.5, V=24, R=24.5, *i*=23.

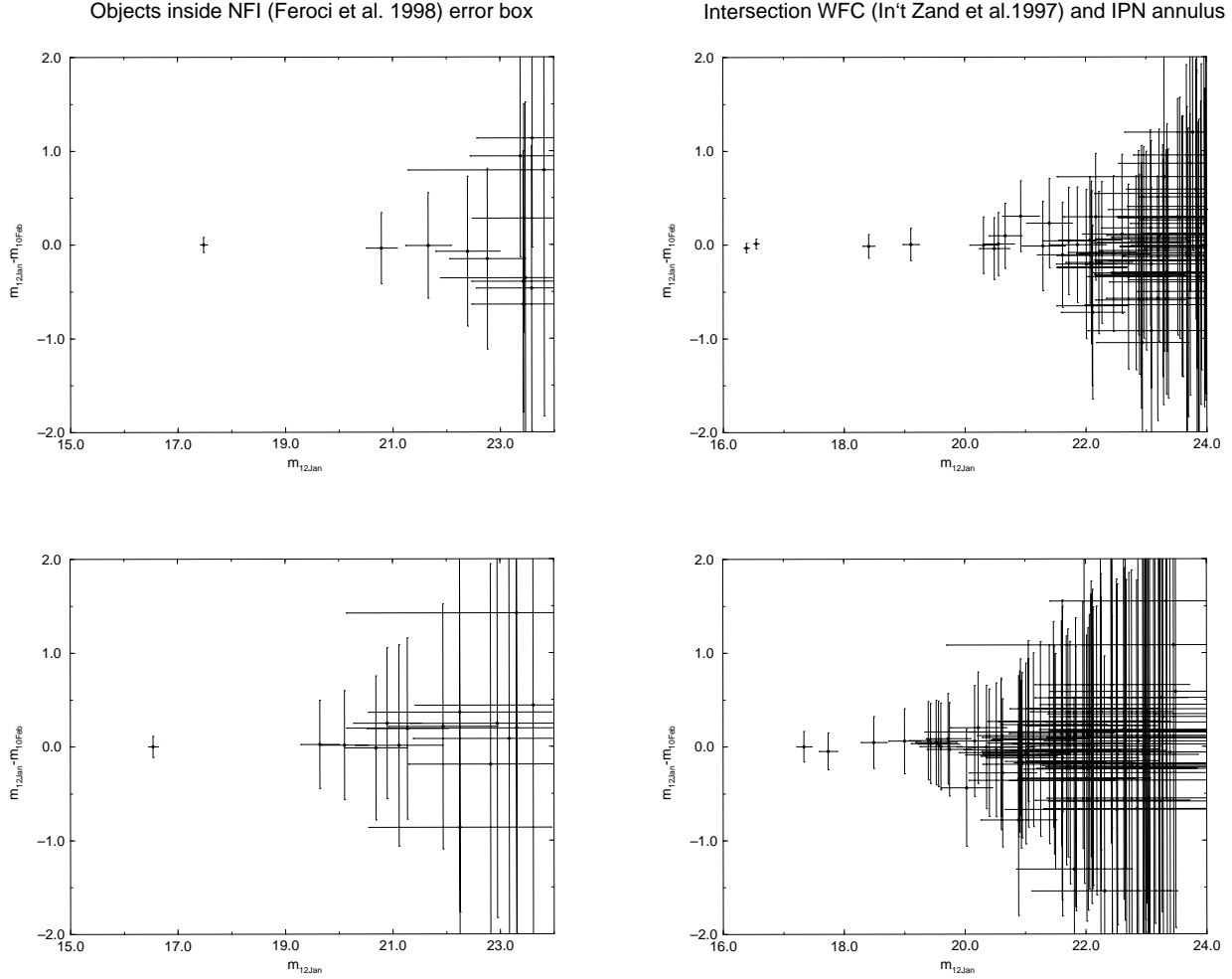


Fig. 3. Δm vs m diagram. The upper two figures show the B magnitude difference for the objects in the frames taken with the 2.2-m Calar Alto telescope 19 hours and 1 month after the gamma-ray emission versus the magnitude, for the different error boxes considered. The lower two images represent the same diagram for the R filter. As it is shown there are no objects varying by more than 1σ .

Using these three sets of observations (CAHA, Loiano, and La Silla) we searched for variable objects inside four different error boxes reported for GRB 970111; i) the WFC error box with a radius of $3'$ (in't Zand et al. 1997), ii) the intersection of i) with the improved IPN annulus (Galama et al. 1997b), iii) the intersection of the reduced WFC error box (Heise et al. 1998) with the improved IPN annulus, and iv) the position given by the NFI error circle for the possible X-ray afterglow (Feroici et al. 1998). For clarity Fig. 3 only shows the above mentioned results for ii) and iv). Colour-colour diagrams were also constructed for the content of the former regions. Automatic photometry was carried out with SEXtractor (Bertin and Arnouts 1996) in the different error boxes reported for GRB 970111.

3. Results

3.1. Search for variable objects

We compared the images taken at CAHA on January 12 with the ones obtained on February 10 and 11. Variable sources have neither been found within the X-ray error boxes of 1SAX J1528.8+1944 and 1SAX J1528.8+1937, nor in the whole $16'$ diameter field.

Fig. 3 shows the magnitude differences in the B and R filters for objects inside the error boxes of GRB 970111 when the frames taken in CAHA 19 hours after the burst and ~ 1 month later are compared. If a suspected variable object is found, it is compared to the images taken at Loiano and La Silla. As it is shown there is no object varying by more than 1σ neither in the R nor in the B filter observations, as reported elsewhere (Castro-Tirado et al. 1997). Furthermore, none of the objects within the different GRB 970111 error box has changed in brightness in the images taken at Loiano and La Silla.

The fields of both X-ray sources 1SAX J1528.8+1944 and 1SAX J1528.8+1937 were observed at Loiano and CAHA us-

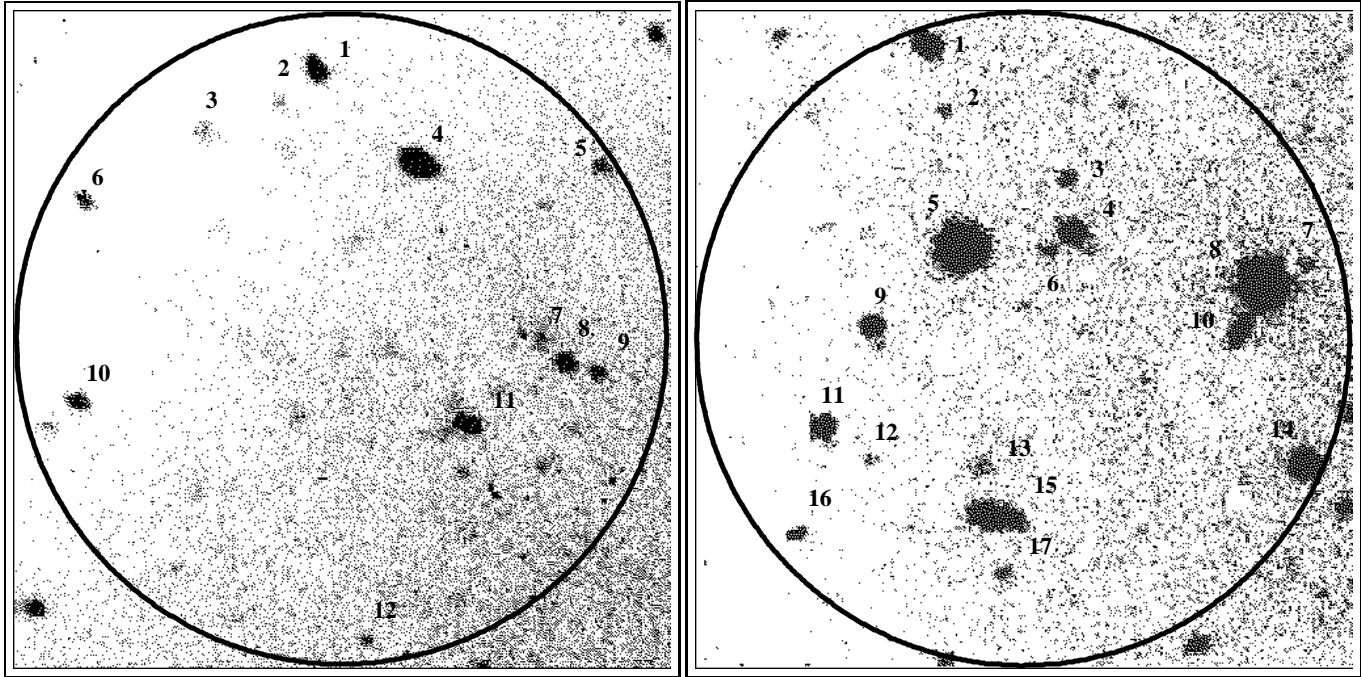


Fig. 4. The error boxes of X-ray sources 1SAX J1528.8+1944 (left) and 1SAX J1528.8+1937 (right) as seen through the B filter in the images taken at Calar Alto on January 12 1997. The field of view is $2' \times 2'$ for both images. The circles represent the 3σ confidence error boxes with a radii of $1'$. The magnitudes of the sources inside the X-ray error boxes are displayed in Tables 6 and 7. North is at the top and east to the left.

ing B and R filters. No variations in brightness were found for any of the objects within the two X-ray sources error boxes. Fig. 4 shows the field of both sources in the B-band.

3.2. Search for the optical counterparts of 1SAX J1528.8+1944 and 1SAX J1528.8+1937

B and R magnitudes for the objects inside the X-ray error boxes of 1SAX J1528.8+1944 and 1SAX J1528.8+1937 are shown in Tables 6 and 7. For objects with magnitudes fainter than 23.5 in B and 22.5 in R, the errors introduced by the photometry do not allow to get reliable values of the B-R colour index. Thus, in

Table 5. Magnitudes of the nine secondary standard stars shown in Fig. 2

Star ID. number in Fig. 2	U	B	V	R	i
1	17.52	17.49	16.86	16.47	16.11
2	16.18	16.06	15.39	15.00	14.63
3	16.14	15.92	15.18	14.76	14.36
4	17.36	17.32	16.67	16.27	15.88
5	18.04	17.32	16.37	15.81	15.29
6	17.47	16.48	15.45	14.84	14.33
7	16.29	16.24	15.59	15.20	14.84
8	17.18	17.29	16.82	16.48	16.15
9	17.09	16.70	15.92	15.48	15.10

Table 6. Magnitudes for objects inside the X-ray error box of 1SAX J1528.8+1944.

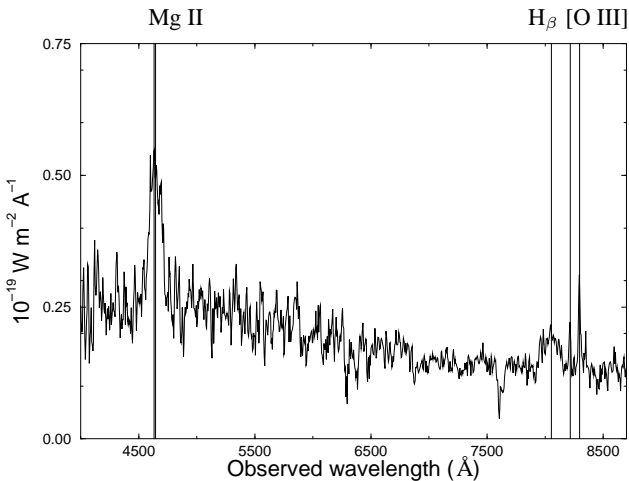
Object	1SAX J1528.8+1944	
	B	B-R
1	21.2 ± 0.5	2.0 ± 0.5
2	23.1 ± 1.1	1.7 ± 1.3
3	22.5 ± 0.6	1.6 ± 0.7
4	20.3 ± 0.3	1.3 ± 0.3
5	22.4 ± 0.9	1.4 ± 1.0
6	22.0 ± 0.9	2.3 ± 0.9
7	22.5 ± 0.7	-0.1 ± 0.9
8	21.9 ± 0.6	1.2 ± 0.7
9	22.4 ± 0.8	2.3 ± 0.8
10	22.0 ± 0.7	1.2 ± 0.8
11	21.1 ± 0.5	1.9 ± 0.6
12	23.4 ± 1.2	1.8 ± 1.4

Tables 6 and 7 only objects brighter than the above mentioned magnitudes are shown.

Object # 11 of Table 6 is coincident with the radio source VLA 1528.7+1945 and has been proposed as the optical counterpart of 1SAX J1528.8+1944 (Frontera et al. 1997, Guarnieri et al. 1997b, Masetti et al. 1997a). This object consists of a blend of at least 2 galaxies with different redshifts (Kulkarni et al. 1997) and shows a fuzzy and complicated structure. The B and R magnitudes reported for object # 11 comprises the flux of all its components. This fact explains the discrepancy of the B

Table 7. Magnitudes for objects inside 1SAX J1528.8+1937 X-ray error box.

1SAX J1528.8+1937		
Object	B	B-R
1	20.0 ±0.2	2.1 ±0.4
2	23.5 ±1.3	1.4 ±1.9
3	23.1 ±1.0	1.3 ±1.1
4	20.6 ±0.3	0.3 ±0.4
5	19.6 ±0.2	1.1 ±0.2
6	22.8 ±1.1	1.7 ±1.2
7	23.2 ±1.2	2.0 ±1.3
8	17.4 ±0.1	1.0 ±0.1
9	21.0 ±0.4	2.1 ±0.4
10	21.8 ±0.6	1.3 ±0.6
11	21.2 ±0.4	1.6 ±0.5
12	23.3 ±1.2	2.3 ±1.2
13	22.5 ±1.1	0.6 ±1.2
14	19.6 ±0.2	1.8 ±0.2
15	20.2 ±0.3	0.8 ±0.3
16	22.5 ±0.9	0.6 ±1.0
17	22.9 ±1.0	0.8 ±1.2

**Fig. 5.** The spectrum of object #4 obtained with 2.2-m (+CAFOS) telescope at Calar Alto. The spectrum has been flux calibrated with an instrumental response determined in a photometric night a few days later. The redshift has been determined to be $z = 0.657 \pm 0.001$ from the narrow emission lines of [O III] 4959, 5007. The broad absorption feature at 7610 Å is the atmospheric A-band.

and R magnitudes with those reported by Kulkarni et al. (1997). We also note object #7 inside error box (Table 6) which shows B-R=-0.1. However the large error in the colour index makes this candidate less likely to be related to 1SAX J1528.8+1944.

We would like to remark that one of the objects in the 1SAX J1528.8+1937 field (object #4, Table 7) is the bluest one with B < 21 found in the 8' radius CAHA image. Two optical spectra of this object were taken with CAFOS at the 2.2-m telescope

of CAHA using the B200 grism (3500-6500 Å) and the R200 grism (6500-10000 Å). The resolution is about 12 Å, given by the 1.25'' slit. Exposure time was 600 sec in B200 and 1200 sec in R200.

Fig. 5 shows the spectrum of object #4, revealing it as a typical Seyfert-1 galaxy with broad emission lines of Mg II (2795.5, 2802.7 Å) and H β (4861 Å), and the narrow emission lines of [O III] (4959 Å, 5007 Å) observed at wavelengths of 8216 Å and 8298 Å. The broad Mg II line is observed at a central wavelength of 4636 Å, which is very consistent with the redshift determined from the narrow lines. The FWHM of the Mg II and H β lines imply internal velocities of $v \approx 7500$ km s $^{-1}$ and $v \approx 4600$ km s $^{-1}$, respectively.

The spectrum was flux calibrated using instrumental responses determined in a photometric night several days later. Taking into account an interstellar absorption of ~ 0.2 mag at ~ 750 nm derived from the reddening (see §3.3) and using the flux level taken from the spectrum, we determine the blue rest-frame luminosity of this AGN to be between $M_B = -21.6$ and $M_B = -22.5$ depending on cosmology ($q_0 = 0.1$, $H_0 = 75$ km s $^{-1}$ Mpc $^{-1}$ and $H_0 = 50$ km s $^{-1}$ Mpc $^{-1}$, respectively).

Cumulative surface densities of quasars/Seyfert-1 have been determined observationally by several authors (Hartwick and Schade 1990, Hawkins and Veron 1995). These authors report the number of quasars and Seyfert-1 galaxies with B < 21 and $z < 2.2$ to be about 30 per square degree, rather independent on the selection criteria employed. Therefore, in our 1' radius X-ray error box the *a priori* probability for finding a quasar or Seyfert-1 galaxy with B < 21 and $z < 2.2$ is roughly 2.7 %. Since object #4 has B=20.6, this probability represents an upper limit. For this reason, we propose object #4 as the optical counterpart of the X-ray source. Astrometry of object #4 yields: $\alpha = 15^h 28^m 47.7^s \pm 0.14^s$, $\delta = 19^\circ 38' 53'' \pm 2''$ (equinox J2000).

3.3. Colour-colour diagrams

In order to detect any object with peculiar colours, colour-colour diagrams were constructed for all objects inside the WFC error box. We consider the error box reported by in't Zand et al. (1997), in order to assure that the possible error boxes are included. For 157 objects inside the above mentioned error box we were able to measure the B, V, R and i magnitudes, that enabled us to construct a B-R vs V-i diagram (see Fig. 6a). Many objects (~ 300) were only detected in the R and B bands.

In order to distinguish objects with colours not expected in stars and normal galaxies, we constructed a colour-colour diagram based on the unreddened colours of 5138 stars of the solar neighbourhood from the catalogue compiled by Lanz (1986), which we have represented by a dotted band in the colour-colour diagram. This band is composed by main sequence, giants and super-giants stars. All the objects with error bars not overlapping with the band are candidates to high-redshift galaxies, quasars, active galactic nuclei or whatever object with an optical emission different from that of normal stars in our galaxy. We have also overplotted the colours for GRB 970508

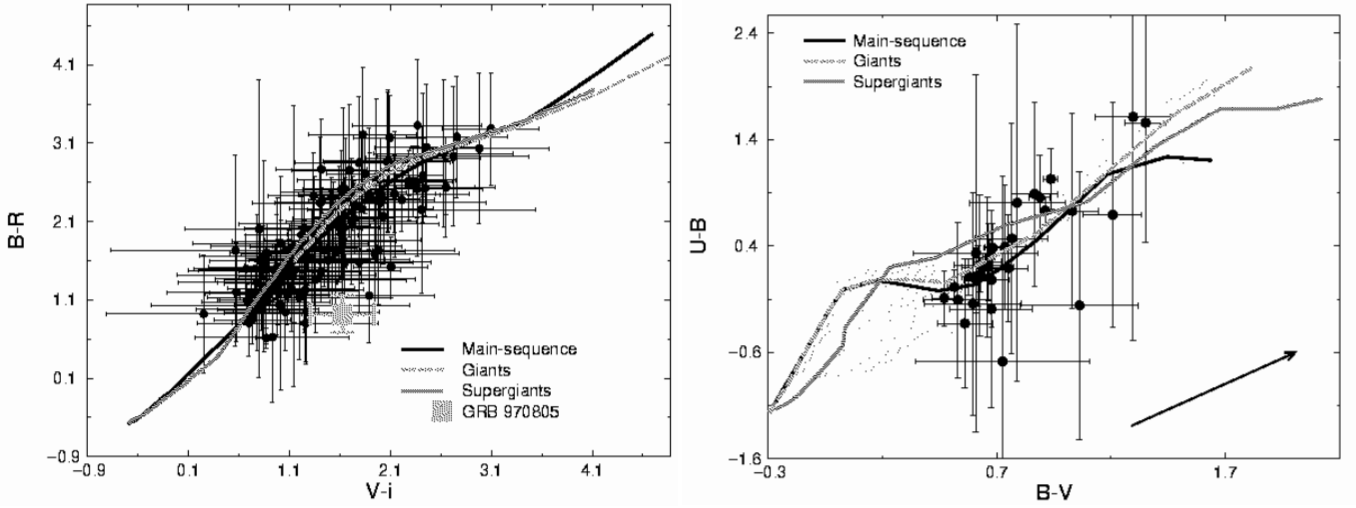


Fig. 6. Colour-colour diagrams for the objects inside the WFC error box. In the left-hand panel there is a B-R vs V-i colour-colour diagram for the 157 objects in the WFC error box for which B,V,R and i measurements were possible. As reference, we have plotted (*big square*) the colours of the GRB 970508 host-galaxy from Zharikov et al. (1998). In the right-hand panel the U-B vs B-V colour-colour diagram is shown for the 31 objects. In both figures the dots represent the colour of real stars taken from a photometric catalogue (Lanz 1986). The different lines show the colours expected for main sequence, giant and supergiant stars. The arrow indicates the reddening direction.

derived from the BVR_cI_c photometry performed from Zharikov et al. (1998). The R filter photometric calibration carried out from Schaefer et al. (1997) and the offsets between Johnson and Kron-Cousins filters (Frei and Gunn 1994) were taken into account. As it is shown, the colours of GRB 970508 are clearly away (at least 2σ) from the band that represents the main sequence stars.

In spite of the larger errors derived from the observations in the U filter in comparison to the other filters, we constructed the U-B vs B-V diagram in order to distinguish objects with ultraviolet excesses, but U,B,V,R and i magnitudes are available only for 31 objects (see Fig. 6b).

The uncertainties for the colour indices were calculated from:

$$\sigma(U - B) = (\sigma(U)^2 + \sigma(B)^2)^{1/2}$$

$$\sigma(B - V) = (\sigma(B)^2 + \sigma(V)^2)^{1/2}$$

$$\sigma(B - R) = (\sigma(B)^2 + \sigma(R)^2)^{1/2}$$

$$\sigma(V - i) = (\sigma(V)^2 + \sigma(i)^2)^{1/2}$$

The colour excess $E(B-V)$ of the objects is related to the Hydrogen column density following Bohlin et al. (1978):

$$E(B-V) = 2.08 \times 10^{-22} N(\text{HI}) \text{ cm}^{-2}$$

The column density along the line of sight of the field ($b^{\text{II}} = 53.4^\circ$) is $N(\text{HI}) \sim 4.8 \times 10^{20} \text{ cm}^{-2}$, which implies a colour excess $E(B-V) \sim 0.1$. Once $E(B-V)$ is known the colour excess for the others filters can be obtained following Cardelli et al. (1989), resulting; $E(U-B) \sim 0.08$, $E(B-R) \sim 0.15$, $E(V-i) \sim 0.13$. Thus the reddening is comparable to the errors on the

photometry. Furthermore, taking into account that the distance of the sources are unknown, we will consider the colour-colour diagrams as the intrinsic colour-colour diagrams for the objects in the field. Fig. 6 shows both diagrams. As it is shown in the colour-colour diagrams, there are no sources that deviate over more than a 2σ level from the colours expected for the usual components of the galaxies (main-sequence, giants or supergiants stars).

Among the 31 objects inside the WFC error box for which four colours are available, there are no sources bluer than $U-B < -0.70$, $B-R < 0.60$, $B-V < 0.45$, $V-R < 0.32$ and $R-i < 0.17$.

3.4. Photometric classification of objects inside the WFC error box, and estimation of their redshift

In order to determine the identity of the objects in the WFC error box, we used a supervised classification method that was originally developed for the Calar Alto Deep Imaging Survey (CADIS) and is used for object classification and accurate redshift estimation of galaxies and quasars there (Wolf et al. 1998a). This method calculates likelihoods for each individual object to resemble either a star, a galaxy or a quasar, based on a comparison of its observed colours with libraries of template colours.

These colour libraries have been calculated from spectral libraries by synthetic photometry based on the UBVRi filter-set and the system responses. As an input, we used the Gunn & Stryker (1983) catalogue of stellar spectra, the galaxy template spectra of Kinney et al. (1996) and a quasar model library derived from the quasar template spectrum of Francis et al. (1991), which is detailed in Wolf et al. (1998b). Since the

galaxy and quasar libraries are parameterized in redshift, it is also possible to estimate the redshift for these two classes of objects.

The performance of this supervised multicolour classification strongly depends on the colour information available and, of course, on the choice of good libraries. According to Wolf et al. (1998a), this method detects broad-line AGNs very reliably, and estimates redshifts for galaxies and quasars, which are mostly accurate to within 5%, if seven or more filters are available with photometric accuracies better than 3%, and the above mentioned libraries are used. Given only four or five broad-band colours, redshift estimates are bound to be less reliable, but classification will still distinguish well between stars and galaxies.

As it was explained in § 3.3, for only 31 objects inside the WFC error box UBVRi photometry was possible, while for 157 objects only BVRi magnitudes were measured. In this case, the low number of bands available and the higher photometric errors of the faint objects left many objects unclassifiable. For the set of 31 sources, the proportion between stars, galaxies and unclassifiable objects were: 74% stars, 18% galaxies and 18% unclassifiable objects. For the set of 157 objects the number of unclassifiable objects was higher: 27% stars, 16% galaxies and 56% were not classified. Probably most of the unclassifiable objects in this set are galaxies because the second set is composed for fainter objects than the set of 31 objects, and so the fraction between galaxies and stars should be higher. For twelve objects that were classified as galaxies we were able to roughly estimate their redshift, yielding values in the range of $0.2 < z < 1.4$. None of the classified objects appears unusual in any respect.

3.5. Long term red-variable stars

WX Ser, a Mira-type variable is detected $\sim 5'$ outside the GRB 970111 error box. Its period of is 425.1 days and a maximum magnitude of $V=12.0$ and a minimum of $V<16$. However, comparing the B images we taken on 12-13 March and 15-16 March 1997 to those obtained on July 1997, we found a variability in the B band of $\Delta B \geq 5$ mag, ranging from $B=20.4 \pm 0.1$ to $B < 15.4$. On the other hand, the variable object found by Masetti et al. (1997b) is located outside the field of view of CAFOS and DFOSC, so we cannot provide further measurements.

3.6. Similarities between GRB 970111 and GRB 980329

GRB 980329 is the tenth GRB localized with the WFC on board *BeppoSAX*. The presence of a radio counterpart inside the NFI error box that peaked ~ 3 days after the gamma-ray event (Taylor et al. 1998), enabled the detection of a near infrared and an optical (I and R band) counterpart (Djorgovski et al. 1998c, Klose 1998, Larkin et al. 1998a, 1998b, Palazzi et al. 1998a, 1998b).

GRB 970111 and GRB 980329 are the most intense GRBs detected by the WFC and the GRB monitor (GRBM), showing a prominent emission above 40 keV. In fact, their fluence

in the 50-300 keV range is about more than four times larger than the largest of the other GRBs detected by *BeppoSAX*. On the other hand, they displayed the hardest spectra of the *BeppoSAX* GRBs, showing a hardness ratio (HR) between 0.6 and 0.7 (in't Zand et al. 1998). Therefore, at first sight one could speculate that both GRBs were originated under similar physical conditions and nearer than the other GRBs of the *BeppoSAX* sample.

If this was the case, the optical decay curves should be somehow similar. This fact could give us a clue for explaining the non detectability of GRB 970111 optical transient 19 hours after the gamma-ray event. According to the power law decay of GRB 980329 ($\alpha=1.3 \pm 0.2$) and the magnitude of the GRB 980329 optical transient $R=23.6 \pm 0.2$ 20 hours after the gamma-ray event (Palazzi et al. 1998b), the magnitude 19 hours after the GRB would be $R=23.5$, barely detectable in our images of GRB 970111.

Taking into account the fluence of GRB 971214 and assuming that GRBs resemble standard candles it could imply that both GRBs were originated from a nearby source in comparison to the source that produced GRB 971214 ($z=3.42$). In fact, Palazzi et al. (1998b) suggest that GRB 980329 could be arised from a strongly obscured starburst galaxy at $z \sim 1$.

4. Conclusion

The new WFC and NFI positions reported for GRB 970111 (Heise et al. 1998, Feroci et al. 1998) and the only marginal overlap between the later and the IPN error box, made us to consider the GRB error box as several non overlapping regions which had to be analyzed independently. Any possible fading was < 0.2 mag for objects with $B<21$, $R<20.8$ and < 0.5 mag for those down to $B=23$ and $R=22.6$. No fading object was detected, within the 1SAX J1528.8+1937 and 1SAX J1528.8+1944 error boxes, being any fading < 0.1 mag for objects with $B<21$ and $R < 20.8$.

The colour-colour diagrams constructed for each non overlapping GRB error box show neither objects with unusual colours nor objects with ultraviolet excesses or highly reddened galaxies. The low interstellar extinction in the direction to GRB 970111 makes the colour-colour diagrams similar to the unreddened ones. No objects bluer than $U-B<-0.70$, $B-R < 0.60$, $B-V < 0.45$, $V-R < 0.32$, $R-i < 0.17$ were found inside the different areas studied. A photometric classification and redshift estimation of the objects in the GRB error box revealed no particularly conspicuous object.

On the basis of the the B-R index we have found a possible candidate with $B=20.6$ for the X-ray source detected by SAX, called 1SAX J1528.8+1937 which is the bluest object found in the $8'$ radius image. Spectroscopic observations revealed that it is a Seyfert-1 galaxy at redshift $z = 0.657$. According to previous surveys, the a *priori* probability that a quasar or Seyfert-1 galaxy with $z < 2.2$ and $B<21$ is located by chance inside the $1'$ X-ray error box, is at most $\sim 3\%$. Therefore, we propose the Seyfert-1 galaxy as the source of 1SAX J1528.8+1937.

On other hand, we report the large amplitude found in the variable star WX Ser ($\Delta B \geq 5$ mag) located $\sim 5'$ outside the GRB 970111 error box.

GRB 970111 shows similar characteristics to GRB 980329, being the most intense and showing the hardest spectra of the GRBs detected by *BeppoSAX*. If they also shared a similar optical decay, the magnitude 19 hours after the GRB would be $R=23.5$ (barely detectable in our images of GRB 970111). This fact could explain the lack of detection of the GRB 970111 optical transient.

Acknowledgments

We are grateful to R. Castillo for the help provided at La Silla and to M. de Santos-Lleó for fruitful discussions. This work has been partially supported by Spanish CICYT grant ESP95-0389-C02-02 and by the University of Bologna (Funds for selected research topics). Jochen Heidt and Thomas Seitz acknowledge support by the Deutsche Forschungsgemeinschaft through SFB 328.

References

- Bertin, E., & Arnouts S. 1996, A&AS, 117, 393.
 Bohlin, R.C., Savage, B.D. & Drake, J.F. 1978, ApJ, 224, 132.
 Bond, H.E. 1997, IAU Circ. 6654.
 Butler, R.C., Piro, L., Costa, E. et al. 1997, IAU Circ. 6539.
 Cardelli, J.A., Geoffrey, C.C., & Mathis, J.S. 1989, ApJ, 345, 245.
 Castro-Tirado, A.J., Gorosabel, J., Heidt, J. et al. 1997, IAU Circ. 6598.
 Castro-Tirado, A.J., Gorosabel, J., Benítez, N. et al. 1998a, Sci 279, 1011.
 Castro-Tirado, A.J., Gorosabel, J., Masetti N. et al. 1998b, in: Proceedings on the 4th Compton Symposium, eds: C.D., Dermer, M.S., Strickman, J.D., Kurfess, AIP 410, 1516.
 Costa E., Feroci M., Piro, L. et al. 1997, IAU Circ. 6533.
 Djorgovski, S.G., Metzger, M.R., Kulkarni, S.R. et al. 1997, Nat 387, 876.
 Djorgovski, S.G., Kulkarni, S.R., Odewahn, S.C., & Ebeling, H. 1998a, GCN 114.
 Djorgovski, S.G., Kulkarni, S.R., Odewahn, S.C., & Ebeling, H. 1998b, GCN 117.
 Djorgovski, S.G., Kulkarni, S.R., Sievers, J., Frail D.A., & Taylor, G. 1998c, GCN 41.
 Feroci, M., Antonelli, L.A., Guainazzi, M. et al. 1998, A&A 332, L29.
 Frail, D.A., Kulkarni, S.R., Costa, E. et al. 1997, ApJ 483, L91.
 Frail, D.A., Halpern, J.P., Bloom, J.S., Kulkarni, S.R. & Djorgovski, S.G. 1998, GCN 128.
 Francis, P. J., Hewett, P.C., Foltz, C.B. et al. 1991, ApJ 373, 465.
 Frei, Z., & Gunn, J.E., 1994, AJ 108, 1476.
 Frontera, F., Costa, E., Piro, L. et al. 1997, IAU Circ. 6567.
 Galama, T., Strom, R., van Paradijs, J. et al. 1997a, IAU Circ. 6571.
 Galama, T., Groot, P.J., Strom, R.G. et al. 1997b, ApJ 486, L5.
 Gorosabel, J., Castro-Tirado, A.J., Willott, C.J. et al. 1998, A&A 335, L5.
 Groot, P.J., Vreeswijk, P.M., Pian, E. et al. 1998, IAU Circ. 6852.
 Guarnieri, A., Bartolini, C., Masetti, N. et al. 1997a, A&A 328, L13.
 Guarnieri, A., Bartolini, C., Piccioni, A. et al. 1997b, IAU Circ. 6544.
 Gunn, J. E., & Stryker, L. L. 1983, ApJS 52, 121.
 Halpern, J., Thorstensen, J., Helfand, D. et al. 1997, IAU Circ. 6788.
 Hartwick, F.D.A., & Schade, D., 1990, A&AR 28, 437.
 Hawkins, M.R.S., & Veron, P., 1995, MNRAS 275, 1102.
 Heise, J. et al. 1998, in: "Gamma-ray Bursts", proceedings on the 4th Huntsville Symposium, eds: C.A. Meegan, R. Preece, T. Koshut, AIP, in press.
 Hjorth, J., Andersen, M.I., Pedersen, H., Jaunsen, A.O., Costa, E. et al. 1998, GCN 109.
 Hurley, K., Kouveliotou, C., Fishman, G., Meegan, C. 1997a, IAU Circ. 6545.
 Hurley, K., Kouveliotou, C., Fishman, G., Meegan, C., & van Paradijs, J. 1997b, IAU Circ. 6571.
 in't Zand, J.J.M., Heise, J., Hoyng, P. et al. 1997, IAU Circ. 6569.
 in't Zand, J.J.M., Amati, L., Antonelli, L.A. et al. 1998, ApJ, submitted.
 Jaunsen, A.O., Hjorth, J., Andersen, M.I. et al. 1998, CGN 74.
 Kinney, A. L., Calzetti, D., Bohlin, R.C. et al. 1996, ApJ 467, 38.
 Klebesadel, R.W., Strong, I.B., & Olson, R.A. 1973, ApJ 182, L85.
 Klose, S. 1998, GCN 43.
 Kulkarni, S.R., Metzger, M.R., & Frail, D.A. 1997, IAU Circ. 6559.
 Kulkarni, S.R., Djorgovski, S.G., Ramaprakash, A.N. et al. 1998, Nat 393, 35.
 Landolt, A.U. 1992, AJ 104, 340.
 Lanz, T. 1986, A&AS 65, 195.

- Larkin, J., Ghez, A., Djorgovski, S. et al. 1998a, GCN 44.
Larkin, J., Ghez, A., Djorgovski, S. et al. 1998b, GCN 51.
Masetti, N., Bartolini, C., Guarnieri, A., & Piccioni, A. 1997a, in: "Cosmic physics in the year 2000", Scientific perspectives and new instrumentation', Soc. It. Fis. Conf. Proc. n.58, p.11.
Masetti, N., Bartolini, C., Guarnieri, A., & Piccioni, A. 1997b, Inf. Bull. Var. Stars Budapest, No. 4440.
Maury, A., Albanese, D., Böer, M., & Feroci, M. 1998, IAU Circ. 6913.
Metzger, M.R., Djorgovski, S.G., Kulkarni, S.R. et al. 1997, Nat 387, 878.
Narayan, R., Paczyński, B. & Piran, T. 1992, ApJ 395, L83.
Palazzi, E., Masetti, N., Pian, E., et al. 1998a, GCN 48.
Palazzi, E., Pian, E., Masetti, N. et al. 1998b, A&A submitted.
Ramaprakash, A.N., Kulkarni, S.R., Frail, D.A. et al. 1998, Nat 393, 43.
Schaefer, B., Schaefer, M., Smith, P. et al. 1997, IAU Circ. 6658.
Smith, I.A., Gruendl, R.A., Liang, E. P., & Lo K.Y. 1997, ApJ 487, L5.
Taylor, G.B., Frail, D.A., Kulkarni, S.R. et al. 1998, GCN 40.
van Paradijs, J., Groot, P.J., Galama, T. et al. 1997, Nat 386, 686.
Voges, W., Boller T., & Greiner J. 1997, IAU Circ. 6539.
Wolf, C., et al. 1998a, in: "Widefield surveys in cosmology", proceedings of IAP98, in preparation.
Wolf, C., et al. 1998b, A&A in preparation.
Zapatero-Osorio, M.R., Castro-Tirado, A.J., Gorosabel, J., Oscoz, A., Kemp, S. et al. 1998, IAU Circ. 6967.
Zharikov, S.V., Sokolov, V.V., & Barysher, Yu.V. 1998, (Astro/ph 9804309).